Journal of Asian Concrete Federation

journal homepage: https://jacf.sfulib3.publicknowledgeproject.org/index.php/jacf

Influence of Permeability and Chloride Ion Binding Capacity on Steel Corrosion in Fly Ash-Based Geopolymers

Chikako Kamei [a,*], Daishin Hanaoka [b]

[a] *Kanazawa Institute of Technology Graduate School, Yatsukaho, Hakusan City, Ishikawa Prefecture, Japan.*
[b] *Kanazawa Institute of Technology, Yatsukaho, Hakusan City, Ishikawa Prefecture, Japan.*

A B S T R A C T

Geopolymers (GP) are concrete alternatives that utilize industrial by-products such as fly ash (FA) and ground granulated blast furnace slag (GGBS) as precursors, significantly reducing CO_2 emissions compared to ordinary Portland cement (OPC). However, the chloride threshold for corrosion initiation in GP remains unclear, hindering their practical adoption. Corrosion of the embedded steel was observed in GP with a chloride ion concentration of 1.0 kg/m^3, but not at 0.4 kg/m^3, indicating that the threshold for mixtures with 10-20% GGBS replacement was between 0.4 and 1.0 kg/m^3. Comparative analysis of OPC concrete and FA-based GP revealed that differences in pore structure, pH at the reinforcement depth, and chloride binding capacity contribute to the higher susceptibility of GP to corrosion. Specifically, GP exhibited higher permeability, lower alkalinity, and negligible chloride binding compared to OPC.

Keywords: Geopolymer, Steel corrosion, Chloride ion, Fly ash, Blast furnace slag

1. Introduction

Geopolymers (GP) are construction materials synthesized from industrial byproducts such as fly ash (FA) and ground granulated blast furnace slag (GGBS) as precursors, offering advantages including reduced CO_2 emissions and valorization of waste materials (Japan Concrete Institute, 2017), while achieving compressive strength comparable to or exceeding that of conventional concrete.

Regarding reinforcement corrosion in GP, previous studies report varied findings. Sato et al. (2016) observed only minimal rib corrosion after 330 days of atmospheric exposure with a chloride concentration of 2.4 kg/m^3. Eitoku et al. (2021) reported no corrosion in FA-based GP concrete after two years in a saline environment, with a chloride ion concentration at the reinforcement of approximately 2.2 kg/m^3. The authors (Hanaoka et al. 2021) demonstrated that under wet-dry cycling using a 3% NaCl solution, the corrosion rate of steel bars in GP may exceed that in OPC. Furthermore, tests using a 10% NaCl solution indicated a reduction in corrosion area with increasing GGBS content, with corrosion initiating at chloride concentrations of at least 3.7 kg/m^3 in mixes with 20% GGBS (Hanaoka et al. 2023). Thus, although knowledge is accumulating, the chloride threshold for corrosion initiation in GP has not been conclusively established. Recent studies suggest that incorporating waste glass powder into recycled or lightweight aggregate concrete can improve resistance to chloride-induced corrosion in marine environments (Peng et al. 2023, Jia et al. 2025).

This study employed two experimental approaches to investigate reinforcement corrosion: outdoor exposure tests and chloride migration tests. In the outdoor exposure tests, mortar specimens were exposed to natural weathering, after which pore volume, permeability, and pH were measured. In the chloride migration tests, chloride ions were supplied externally. When corrosion was suspected, specimens were dismantled to inspect for corrosion, and the chloride concentration at the reinforcement was measured.

2. Methodology

2.1. Materials and Mix Proportions

*Corresponding author: Chikako Kamei (c6400756@st.kanazawa-it.ac.jp)

DOI http://dx.doi.org/10.18702/acf.2026.12.1.51

Received: 27-Oct-2025; Revised: 21-Jan-2026; Accepted: 23-Jan-2026; Published online: 31-March-2026

ISSN 2465-7964, eISSN 2465-7972.

Materials used are listed in Table 1. The alkaline activator consisted of a sodium hydroxide solution (3.6 mol/L) and J-type sodium silicate No. 1 (water glass). The precursors were JIS A 6201 Fly Ash Type II and JIS A 6206 Blast Furnace Slag Micro powder 4000 (without gypsum). Three mixes were prepared (Table 2): OPC, GGBS10, and GGBS20. The OPC mortar had a water-cement ratio of 0.48. The GP mortars, GGBS10 and GGBS20, were derived from a standard GP concrete mix (Japan Society of Civil Engineers 2022), omitting coarse aggregate while maintaining the volumetric ratios of the other constituents to isolate binder effects. The ratio of alkali silicate solution volume (L) to precursor (P) mass was 0.9. GGBS replaced 10% and 20% of the FA by mass, respectively.

Specimens were cured in a sealed environment at 20° C and 60% R.H. for 28 days, as prior studies showed no significant difference in 28 days compressive strength between heated and sealed curing for GGBS-containing GP (Japan Society of Civil Engineers 2022, Kamei et al. 2024). The 28 days compressive strengths were 32.5 MPa for OPC, 28.3 MPa for GGBS10, and 41.3 MPa for GGBS20. The OPC and GGBS10 exhibited comparable strengths, while GGBS20 was significantly higher, consistent with previous findings (Japan Society of Civil Engineers 2022).

Table 1. Materials used

Category	Symbol	Materials	Density (g/cm^3)	Specific surface area (cm^2/g)	Water absorption rate(%)
Sodium hydroxide solution	SH	Solution of NaOH prepared by dissolving granular reagent-grade NaOH in distilled water to a concentration of 3.6 mol/L.	1.14	-	-
Water glass	SS	J Silica Soda No. 1	1.70	-	-
Precursors	FA	JIS A 6201 Fly Ash Type II	2.24	3530	-
	GGBS	JIS A 6206 Blast Furnace Slag Micro powder 4000 (No Gypsum)	2.91	3980	-
Fine aggregate	S	River sand (Coarse grain rate 3.13)	2.58	-	2.27
Water	W	Tap water	1.00	-	-

Table 2. Mix proportions and compressive strength

Formulation Name	GGBS/P (%)	L/P	SS/SH	Unit Amount (Upper: kg/m^3 Lower: L/m^3) SS	SH	FA	GGBS	S	Air	σ28 Compressive strength (MPa)
GGBS10	10 (8 ol.%)	0.9	1	212	214	715	81	830	0	28.3
				125	188	319	28	321	20	
GGBS20	20 (16 ol.%)			212	214	652	163	830	0	41.3
				125	188	219	56	321	20	

2.2. Specimen Preparation and Exposure

Specimens (100×100×400 mm) were prepared with D13 deformed bars embedded at a cover depth of 50 mm (Fig. 1). These specimens were placed outdoors in Hakusan City, Ishikawa Prefecture, for approximately 23 months starting September 28, 2023 (Fig. 2). To minimize direct rain exposure, specimens were oriented with the cast surface facing downward.

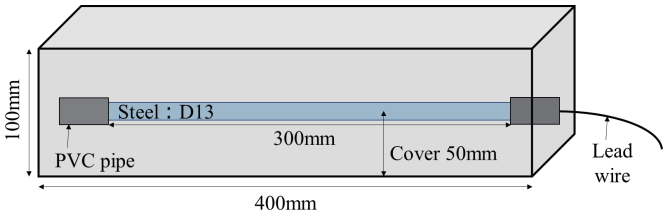

Fig. 1. Outdoor exposure test specimens

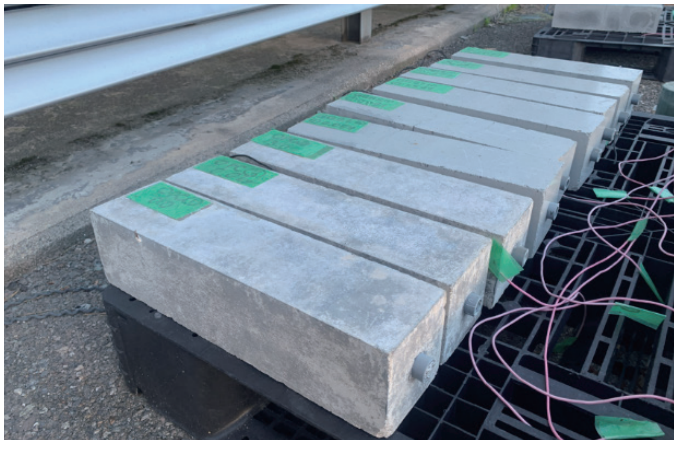

Fig. 2. Outdoor exposure environment

2.3. Pore Structure Analysis

Pore structure was analyzed using mercury intrusion porosimetry (MIP) technique to measure total pore volume and

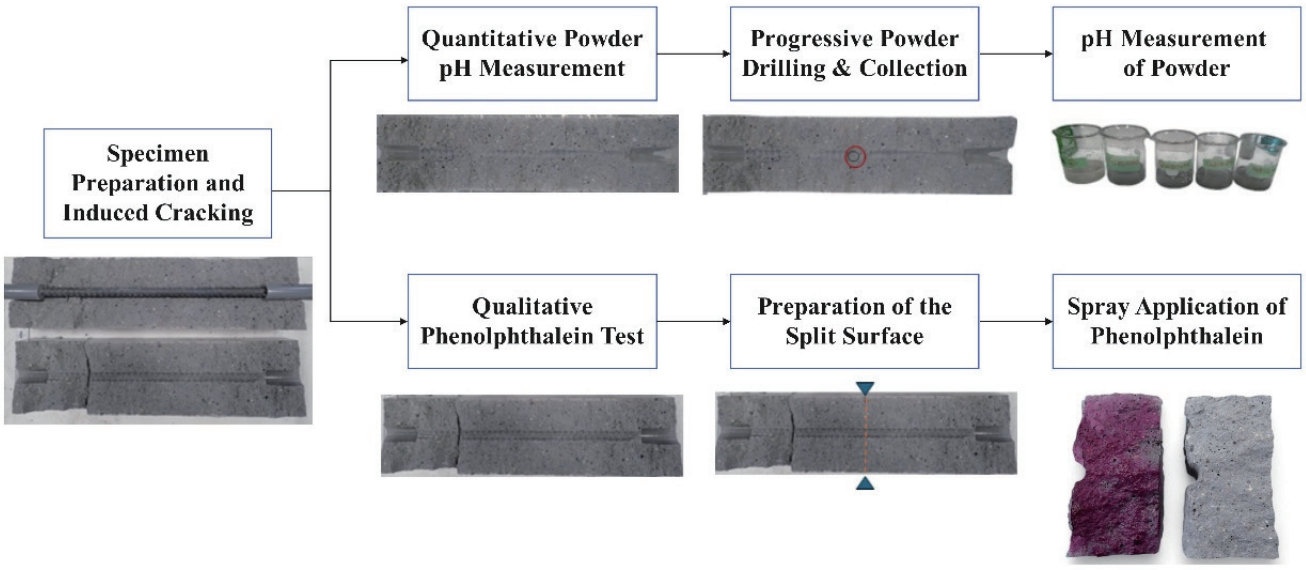

Fig. 3. Process Flow for Combined Phenolphthalein Test and Powder pH Measurement

ink-bottle pore volume. Samples were taken from the center of the specimen (Fig. 1). Samples were crushed to approximately 5 mm, treated with acetone immersion, and vacuum-dried before MIP analysis at a maximum pressure of 124 MPa. In the mercury penetration test, the results obtained from the initial measurement were defined as the total pore volume, while the mercury penetration behavior during the second pressurization and depressurization cycle following the initial measurement was defined as the continuous pore volume.

2.4. Water and Air Permeability Tests

Water permeability and air permeability coefficient tests were conducted on specimens identical to those in Section 2.2. The water head was measured visually, and the air permeability coefficient was determined using the Torrent method. To minimize the influence of local surface defects, permeability measurements were conducted multiple times at locations where no visible cracks were observed. The Torrent method creates a sealed space on the concrete surface, maintaining a constant vacuum pressure within it. It measures how much the pressure changes over a fixed period of time after the air in the surface layer has been evacuated.

2.5. pH Measurement

After three months of outdoor exposure, the specimen was split open and the split surface was sprayed with a 1% phenolphthalein solution to confirm neutralization. Two powder samples were extracted from near the center of a single specimen for each mix proportion that showed no neutralization, and the pH was measured based on previous research (Kaneko et al., 2017). Specifically, the powder was mixed with distilled water to a powder concentration of 1%, and the suspension immediately after stirring was measured with a digital pH meter. The reported value is the average of the two measurements.

2.6. Chloride Migration Test (Reinforcement Corrosion Test)

The chloride migration test followed a previous method (Horiguchi et al., 2015). The specimen dimensions are shown in Fig. 4. Each 100×100×400 mm prism contained two D13 deformed bars with pure covers of 20 mm and 30 mm. A lead reference electrode for natural potential measurement was installed in the specimen center. After 28 days of curing, a chloride ion supply cell was fixed to the test surface. The specimen was dried, coated with epoxy resin on all but two surfaces (labeled in Fig. 4), and saturated in fresh water. The chloride ion supply cell was then filled with a 10% sodium chloride solution. The natural potential was measured every 10 minutes. Specimens were dismantled when a sharp potential drop occurred. Mortar samples were collected from around the bars (Fig. 5) to measure total and water-soluble chloride ion content via potentiometric titration (JIS A 1154).

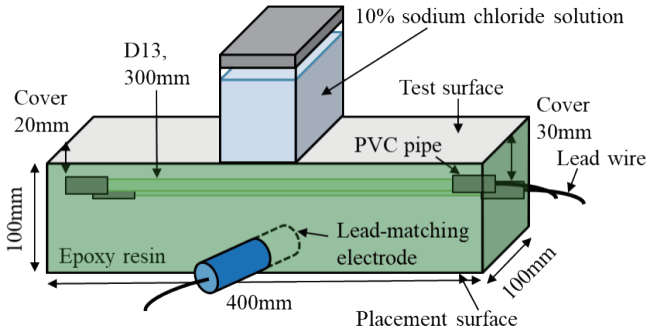

Fig. 4. Chloride migration test setup

3. Results and Discussion

3.1. Pore Structure

Figure 6 shows the results for total pore volume and continuous pore volume. GGBS10 exhibited the highest

volumes for both total and continuous pores. While OPC and GGBS20 had comparable total pore volumes in the 10 – 20 nm range, GGBS20 showed more continuous pores than OPC. This indicates that GP, due to their higher continuous pore volume, allow easier ingress of water and air compared to OPC. The permeable nature of GP can be attributed to their microstructure, which results from a condensation polymerization process that forms a more open framework compared to OPC paste (Ichimiya et al. 2018).

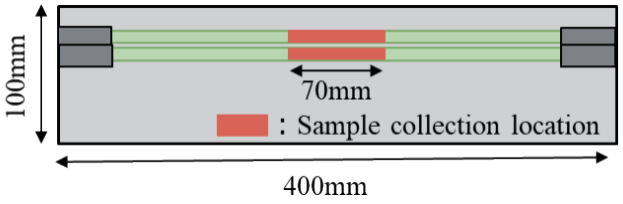

Fig. 5. Sample collection location for chloride analysis

3.2. Water and Air Permeability

Figure 7 shows the water permeability results, and Figure 8 shows the air permeability results. Both permeability and air permeability were higher for the GP than for OPC. GGBS10 exhibited the highest water permeability, consistent with the pore volume results. However, the surface air permeability coefficient was higher for GGBS20 than for GGBS10. As shown in the photograph in Figure 8, the GGBS20 surface exhibited exposed fine aggregates and visible voids, suggesting that the fine surface cracks were responsible for the increased permeability. Previous literature (Ichimiya et al., 2017) has reported that surface degradation of GP is significant in low-temperature, low-humidity environments. It has also been reported that GGBS-added formulations swell upon water absorption, and that the amount of expansion increases with an increase in the GGBS substitution rate. This experiment involved outdoor exposure in winter, and it is thought that surface degradation occurred in GGBS20, which has a high GGBS substitution rate.

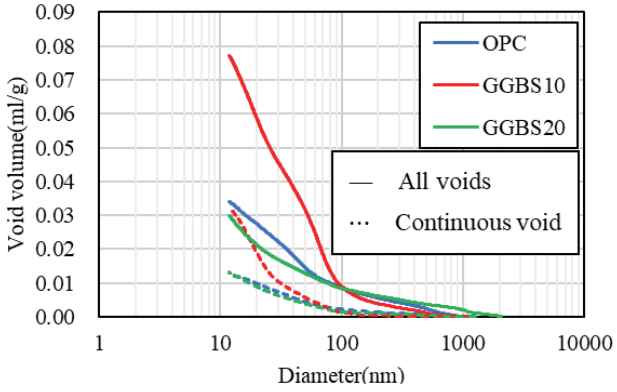

Fig. 6. Total pore volume and continuous pore volume

3.3. pH

The pH measurements after three months of outdoor exposure were 12.3 for OPC, 11.3 for GGBS10, and 11.5 for GGBS20. The pH immediately after mortar mixing was 13.0 for OPC and 13.1 for GGBS20 (GGBS10 not measured). The pH of the GP specimens after outdoor exposure was significantly lower than that of OPC. Although phenolphthalein testing indicated no full carbonation (the sample site turned reddish-brown), the high gas permeability of the GP suggests that carbon dioxide ingress and partial carbonation-like reactions may have occurred more readily than in OPC. Furthermore, the geopolymerization process itself is a dehydration condensation reaction that consumes hydroxyl ions (OH^-) (Japan Society of Civil Engineers, 2022), contributing to a lower stable pore solution pH compared to the portlandite-buffered system in OPC. Given that reinforcement corrosion generally initiates at pH $\leqslant$ 11 (Japan Concrete Institute, 2024), the lower pH environment of GP is more conducive to corrosion initiation.

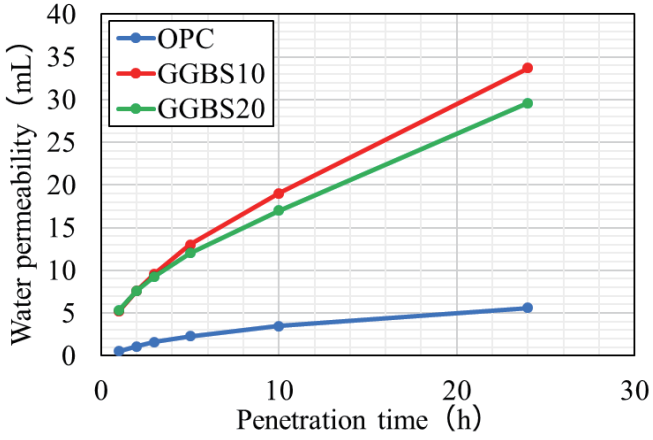

Fig. 7. Water permeability rate

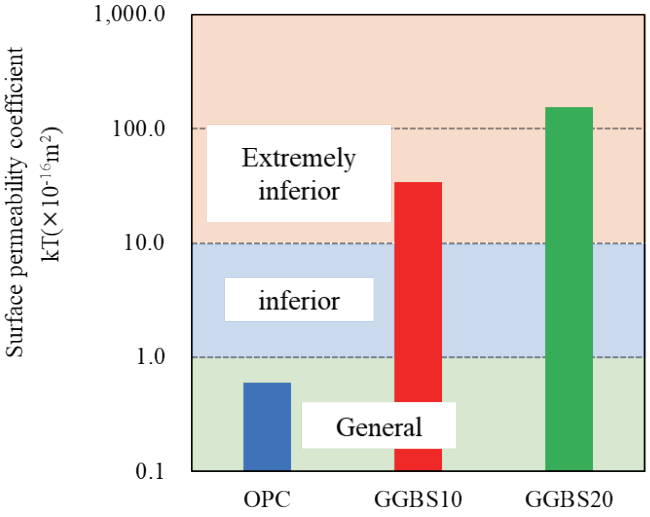

Fig. 8. Surface air permeability coefficient and representative surface conditions

3.4. Chloride Migration and Binding

Figure 9 shows the natural potential measurements. A sharp drop in potential for the 20 mm cover bar occurred

Table 3. Example of specimen disassembly inspection (Chloride migration test)

Formulation Name	Cover 20 mm	Cover 30 mm
OPC		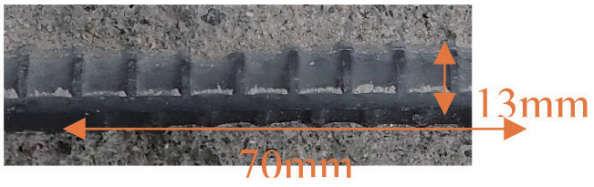
GGBS10		
GGBS20		

○: Location where corrosion of reinforcing bars was confirmed

around 45 days for OPC, between 12 hours and 3 days for GGBS10, and within 2 to 10 days for GGBS20. The significantly shorter time observed with GP is attributed to accelerated chloride ion permeation resulting from their higher water absorption and larger continuous pore volume compared to ordinary Portland cement. The longer time for GGBS20 compared to GGBS10 is attributed to a denser matrix with higher GGBS content (Ismail et al., 2014).

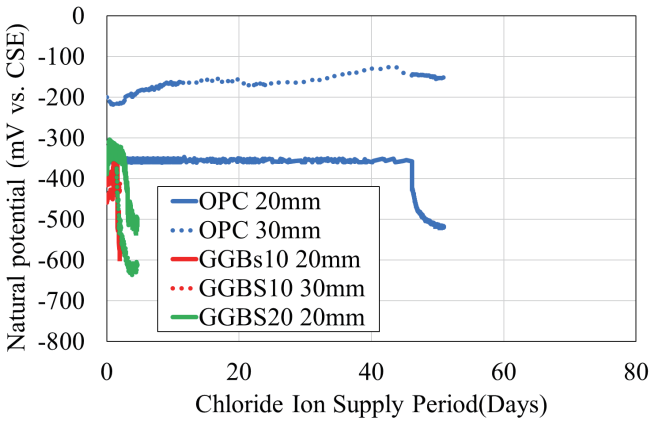

Fig. 9. Natural potential measurement results (chloride migration test)

Table 3 shows examples from the disassembly inspection, and Table 4 summarizes the presence of corrosion and the corresponding total chloride ion concentration. Corrosion of reinforcement in OPC occurred at chloride ion concentrations between 1.8 and 3.9 kg/m^3, while no corrosion was observed at 0.2 kg/m^3, validating previous results (Horiguchi et al., 2015). All reinforcement in GGBS10 specimens corroded (2.2 to 5.3 kg/m^3). For GGBS20, corrosion was confirmed at concentrations between 1.0 and 4.1 kg/m^3, with no corrosion at 0.4 kg/m^3.

Note: The analysis for OPC is based on two specimens. An additional OPC specimen was tested but excluded from the final analysis as a clear potential drop the predetermined trigger for terminating the chloride supply was not unambiguously detected, leading to a non-standardized test duration. All geopolymer specimens yielded interpretable results within the defined test protocol.

Figure 10 shows the water-soluble chloride content and chloride binding capacity. OPC fixed approximately 44% of the total chloride ions, whereas the GP showed almost no chloride binding, consistent with previous research (Uehara et al., 2013). This difference stems from the chemical composition of the precursors. Fly ash (FA) primarily contains Si and Al, while GGBS consists mainly of Si, Al, and Ca (Japan Society of Civil Engineers, 2022). The geopolymerization process consumes available Al_2O_3 (Japan Society of Civil Engineers, 2022), and the system contains only a small amount of calcium. Consequently, the stable phases that form lack the calcium-aluminate-hydrate (C-A-H) frameworks necessary to bind chloride ions as Friedel's salt ($3CaO \cdot Al_2O_3 \cdot CaCl_2 \cdot 10H_2O$), which is common in OPC systems.

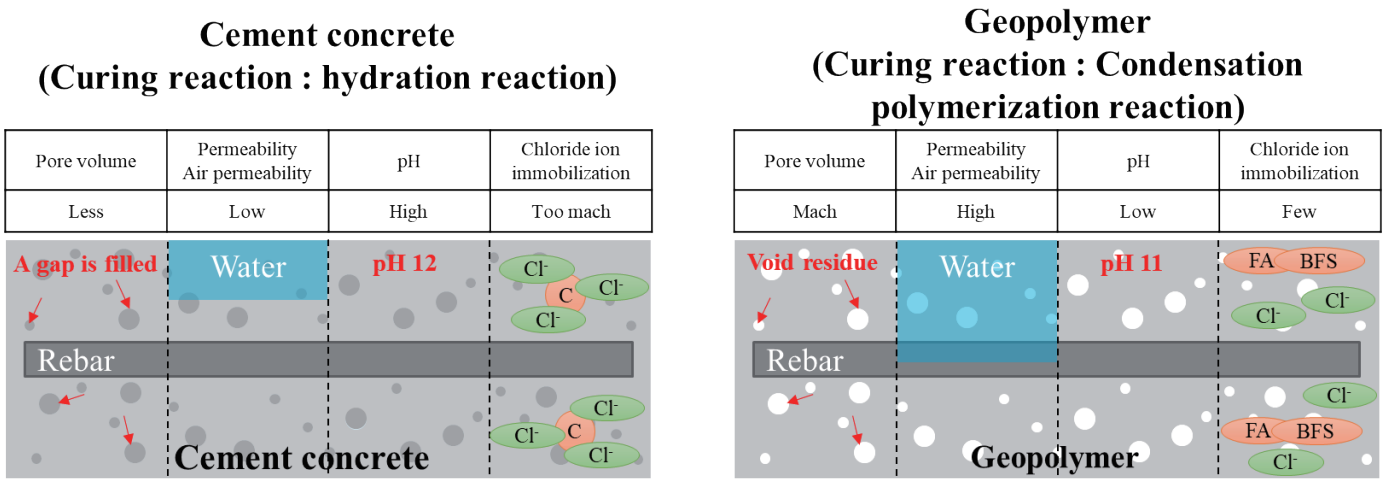

Fig. 11. Comparison of reinforcement corrosion in cement concrete and geopolymers

Table 4. Presence of reinforcement corrosion and total chloride ion concentration

Formulation Name	Number	Cover 20 mm		Cover 30 mm	
		Presence of corrosion	Chloride ion concentration (kg/m^3)	Presence of corrosion	Chloride ion concentration (kg/m^3)
OPC	①	corrosion	3.9	corrosion	1.8
	②	corrosion	2.5	Not corrosion	0.2
GGBS10	①	corrosion	4.1	corrosion	3.6
	②	corrosion	5.3	corrosion	2.2
	③	corrosion	5.1	corrosion	4.0
GGBS20	①	corrosion	4.1	corrosion	1.0
	②	corrosion	3.1	Not corrosion	0.4
	③	corrosion	4.1	corrosion	1.9

Fig. 10. Water-soluble chloride content and chloride binding capacity

4. Summary

The main findings of this study are summarized as follows:

(1). In this experiment, the fly ash-based geopolymer, which uses sodium hydroxide and water glass as alkaline activators, hardens through a dehydration condensation polymerization reaction, and therefore exhibits a larger continuous pore volume and higher permeability to water and air than cement concrete, which hardens through a hydration reaction.

(2). Within the scope of this experiment, the lower pH of geopolymers compared to OPC after outdoor exposure is attributed to a combination of factors: the consumption of OH^- during the geopolymerization reaction and the high permeability which may facilitate carbon dioxide ingress and partial carbonation.

(3). The geopolymer composed primarily of fly ash containing almost no calcium exhibited significantly lower chloride ion binding capacity than ordinary Portland cement, due to the lack of calcium-aluminate phases necessary to form Friedel's chloride ion.

(4). For geopolymer, no corrosion was observed at a chloride ion concentration of 0.4 kg/m^3, but corrosion was observed at 1.0 kg/m^3. This suggests that the critical chloride ion concentration for corrosion of GP steel is between 0.4 and 1.0 kg/m^3. In other words, this indicates that the corrosion initiation threshold is lower than that typically reported for OPC.

In summary, compared to OPC, geopolymers have a lower pH and minimal chloride binding capacity. Consequently, even minor chloride ion ingress can initiate reinforcement corrosion, leading to a shorter initiation period and potentially accelerated corrosion rate. The findings indicate that while FA-based GP presents a higher corrosion risk in chloride environments, its durability profile including acid resistance and refractory properties may be superior in other applications. Therefore, optimizing GP mix design, such as increasing GGBS content for enhanced chloride resistance or leveraging computational mixture design approaches, should be strategically aligned with the intended service environment.

CRediT authorship contribution statement

Chikako Kamei: Conceptualization, Investigation, Writing – original draft.

Daishin Hanaoka: Supervision, Writing – review & editing.

Declaration of competing interest

The authors declare that they have no known competing financial interests or personal relationships that could have appeared to influence the work reported in this paper.

Acknowledgments

Part of this research was supported by a research grant from the Maeda Memorial Foundation for the Advancement of Engineering in fiscal year 2025. The authors express their sincere gratitude for this support.

References

[1] Japan Concrete Institute (2017). "Research Committee Report on the Application of Geopolymer Technology in the Construction Field," Japan Concrete Institute, Tokyo, Japan.
[2] Sato, T. et.al (2016). "Relationships between the Products and pH and Other Properties of Geopolymer Cured Materials in Various Formulations and Preparation Methods," Proceedings of the Japan Concrete Institute, Vol. 38, pp. 2325-2330.
[3] Eitoku, Y. et.al (2021). "Properties of Fly Ash-Based Geopolymer Concrete Exposed to Chloride ion Damage for Two Years," Proceedings of the Japan Concrete Institute, Vol. 43, pp. 1367-1368.
[4] Hanaoka, D. et.al (2021). "Evaluation of Chloride ion Permeability of Geopolymer and Corrosion of Rebar Bars," Proceedings of the Japan Concrete Institute, Vol. 43, pp. 1361-1366.
[5] Hanaoka, D. et.al (2023). "Study on Properties of Geopolymer Concrete and Corrosion of Rebar Bars," Proceedings of the Japan Concrete Institute, Vol. 45, pp. 982-987.
[6] Ligang Peng et.al "Enhancing the corrosion resistance of recycled aggregate concrete by incorporating waste glass powder, "Cement and Concrete Composites, 137, pp.1-13, 2023
[7] Bin Jia et.al "Leveraging waste glass powder in recycled aggregate concrete: Mitigating steel corrosion and corrosion-induced cracking under marine exposure," Construction and Building Materials, 502, pp.1-20, 2025
[8] Japan Society of Civil Engineers (2022). Concrete Library 132: Report of Research Subcommittee for Promoting Practical Application of Geopolymer Technology, Japan Society of Civil Engineers, Tokyo, Japan.
[9] Kamei, C. et.al (2024). "Study on the Corrosion Characteristics of Steel Embedded in Fly Ash-Based Geopolymers," Proceedings of the 2024 Chubu Branch Research Presentation Meeting of the Japan Society of Civil Engineers, Ishikawa, Japan.
[10] Kaneko, Y. et.al (2017). "A Study on a Method for Predicting the Progression of Concrete Carbonation Using Drill Cuttings," Annual Proceedings of the Concrete Engineering Society, Vol. 39, No. 1, pp. 1927-1932.
[11] Horiguchi, K. et.al (2015). "Research on the Measurement Method and Quantitative Evaluation of the Corrosion Initiation Limit Chloride Ion Concentration," Journal of Civil Engineering E2 (Materials and Concrete Structures), Vol. 71, No. 2, pp. 107-123.
[12] Ichimiya, K. et.al (2017). "Fundamental Experiments on Surface Degradation Due to Partial Water Absorption in Fly Ash-Based Geopolymers" Proceedings of the Japan Concrete Institute, Vol. 39, pp. 2047-2052.
[13] Ichimiya, K. et.al (2018). "Current Status and Future Prospects of Geopolymers," Concrete Engineering, Vol. 56, No. 5, pp. 409-414.
[14] Ismail, I. et.al (2014). "Modification of phase evolution in alkali-activated blast furnace slag by the incorporation of fly ash," Cement and Concrete Composites, Vol. 45, pp. 125-135.
[15] Japan Concrete Institute (2024). Concrete Diagnosis Technology '24: Fundamentals, Japan Concrete Institute, Tokyo, Japan, p. 35.
[16] Uehara, M. et.al (2013). "Chloride Ion Permeability of Fly Ash Geopolymer Hardened Bodies," The 68th Annual Conference of the Japan Society of Civil Engin